

# Discrete Bathochromic Shifts Exhibited by Fluorescein Ligand Bound to Rabbit Polyclonal Anti-Fluorescein Fab Fragments

Edward W. Voss Jr.,<sup>1,3</sup> John C. Croney,<sup>2</sup> and David M. Jameson<sup>2</sup>

Received December 27, 2001

Eleven individual hyperimmune rabbit polyclonal anti-fluorescein Fab fragment preparations were resolved into heterogeneous subfractions based on differential dissociation times from a specific adsorbent. Four Fab subfractions (i.e., 0.1-, 1.0-, 10-, and 100-day elutions) that differed in affinity were characterized and classified according to the extent of the bathochromic shift in the absorption properties of antibody-bound fluorescein ligand. Absorption maxima of bound fluorescein were shifted in all cases to two distinct narrow ranges, namely, 505 to 507 nm or 518 to 520 nm relative to 491 nm for free fluorescein. There was no direct correlation between the two spectral shift populations and antibody affinity, fluorescence polarization, fluorescence quenching, or fluorescence lifetimes of bound ligand. Fluorescence emission maxima varied with the bathochromic shift range. Bound fluorescein ligand, with absorption maxima of 505 to 507 nm and 518 to 520 nm showed fluorescence emission maxima of 519 to 520 nm and 535 nm, respectively. The two spectral shift ranges differed by ~14 to 15 nm and/or energies of ~1.5 kcal mol<sup>-1</sup> relative to each other and to the absorption maximum for free fluorescein. Spectral effects on the antibody-bound ligand were discussed relative to solvent-water studies and the atomic structure of a high-affinity liganded anti-fluorescein active site.

**KEY WORDS:** Bathochromic shift; fluorescein; Fab fragments; anti-fluorescein antibodies.

## 1. INTRODUCTION

Fluorophores, either specifically bound or covalently conjugated to biomacromolecules, often exhibit significant intrinsic spectral property changes. Specific effects may include spectral shifts in absorption maxima (e.g., bathochromic) as well as changes in the fluorescence emission spectra, polarizations, quantum yields and/or fluorescence lifetimes of the excited fluorophore (Jameson, 1984; Lakowicz, 1999a). Changes in any or all of these spectral parameters directly convey the resident

microenvironment and/or involvement of the fluorophore in various noncovalent chemical-bonding interactions within a specific binding site of a macromolecule. Due to the complexity of multiple spectral changes acting independently or dependently, it has been difficult to directly correlate specific differences in spectral properties (qualitatively or quantitatively) with biomolecular events. To circumvent these problems investigators have historically resorted to studies of solvent effects on fluorophores in solution in attempts to chemically simulate biological systems (Lakowicz, 1999b). Collectively solvent studies have yielded important information, including mathematical expressions derived to predict spectral changes in terms of molecular interactions occurring

<sup>1</sup> Department of Veterinary Pathobiology, College of Veterinary Medicine, University of Illinois, 2522 Veterinary Medicine Basic Science Building, 2001 South Lincoln Avenue, Urbana, IL 61802, USA.

<sup>2</sup> Department of Cell and Molecular Biology, John A. Burns School of Medicine, University of Hawaii-Manoa, 1960 East-West Road, Honolulu, Hawaii 96822, USA.

<sup>3</sup> To whom correspondence should be addressed. E-mail: e-voss1@life.uiuc.edu

<sup>4</sup> Abbreviations: FITC, fluorescein isothiocyanate; KLH, keyhole limpet hemocyanin; MEK, methyl ethyl ketone; DMF, N, N-dimethylformaldehyde; DTT, dithiothreitol; SDS-PAGE, sodium dodecyl sulfate-polyacrylamide gel electrophoresis; MPD, 2-methyl-2,4-pentandiol; DMSO, dimethyl sulfoxide.

between solvent dipoles and fluorophores (MacGregor and Weber, 1981). However, solvent or water-solvent modeling studies with fluorophores have not accurately simulated the complexity inherent in biological systems due in part to issues of isotropy and symmetry (MacGregor and Weber, 1981; Harris and Bertolucci, 1978).

Anti-fluorescein antibodies represent a unique biological system to study various spectral effects. With the fluorophore as the homologous ligand in specific interactions with antibody active sites, a well-defined system amenable to molecular and spectral characterization awaits. Fluorescein is advantageous in model binding and spectral studies since as a prototypical fluorophore it has been extensively characterized. Significant changes in the spectral properties of fluorescein have been reported under various conditions, providing a comprehensive reference database for comparisons and interpretations (Lindqvist, 1960; Martin and Lindqvist, 1975; Fleming *et al.*, 1977; Sjoback *et al.*, 1995; Magde *et al.*, 1999; Klonis and Sawyer, 1996; Watt and Voss, 1997; Choi and Hawkins, 1995; Martin, 1975; Mummert and Voss, 1995; Bailey *et al.*, 1995; Hadjianestis and Nikokavouras, 1993; Stanton *et al.*, 1984; Yguerabide *et al.*, 1994). For example, spectral properties of fluorescein in the dianion form have been examined in various solvent-water mixtures as a probe of hydrogen bonding environments toward understanding biological systems (Klonis *et al.*, 1998; Klonis and Sawyer, 2000). The magnitude of specific spectral energy changes correlated with the  $\alpha$  and  $\beta$  parameters of Kamlet and Taft (1976) that provided a scale for the hydrogen bond donor acidities and acceptor basicities of solvents.

In this report, Fab fragments derived from a series of rabbit polyclonal IgG anti-fluorescein antibodies<sup>4</sup> were employed to study spectral shifts in the absorption spectrum of antibody-bound fluorescein ligand. Although spectral shifts in absorption have been of general interest to spectroscopists, and have been the focus of extensive research in solvent-based systems (Klonis *et al.*, 1998; Klonis and Sawyer, 2000), more detailed biologically based studies are required to understand the magnitude and importance of such shifts in transition energies. As an example, it is not known what specific biochemical information can be derived from such spectral shifts, and if they correlate with other fluorescence parameters. Thus, the experimental concept invoked was to correlate spectral changes in the fluorescein ligand upon binding to specific antibodies with various fluorescence parameters and properties (e.g., affinity) of the antibody molecules.

Anti-fluorescein antibodies procured after prolonged immunization periods were selectively studied due to previously reported spectral shift patterns produced by fluorescein upon interaction with hyperimmune

antibody populations (Klonis *et al.*, 1998; Voss *et al.*, 2001). First, rabbit polyclonal IgG anti-fluorescein antibodies were selected from the late hyperimmune state since they represented heterogeneous populations that possessed higher affinities ( $10^9$ – $10^{11}$  M<sup>-1</sup>) and larger bathochromic shifts in absorption of bound fluorescein ligand than those measured with other mammalian species (Voss, 1990). Second, purified IgG antibodies were obtained from single bleedings from individual rabbits to avoid population pooling effects. Third, purified IgG antibodies were enzymatically degraded to univalent Fab fragments (50 kDa) to eliminate multiple active site interactions (i.e., avidity) in favor of a subfractionation system solely dependent on bimolecular affinity interactions. Fourth, a unique dissociation rate-dependent subfractionation procedure was developed to subdivide the polyclonal Fab anti-fluorescein antibody population into relatively more homogeneous subsets based on affinity differences (Voss *et al.*, 2001).

The studies demonstrated that high-affinity anti-fluorescein polyclonal antibody populations, resolved into subpopulations, were amenable to the systematic study of bathochromic shifts in the absorption spectrum of bound fluorescein ligand (Voss *et al.*, 2001). Antibody-mediated bathochromic shifts from 491 nm (free fluorescein) fell into one of two equally spaced wavelength ranges. The two discrete spectral shift ranges were related to various excited state phenomena as well as antibody function.

## 2. MATERIALS AND METHODS

### 2.1. Preparation of Fluorescein Immunogen

Fluorescein isothiocyanate (FITC, isomer I), obtained from Molecular Probes Inc. (Eugene, OR), was reacted with keyhole limpet hemocyanin (KLH, Calbiochem, San Diego, CA) using the described protocol. To 100 mg KLH, dissolved in 5.0 ml H<sub>2</sub>O, was added 25 mg potassium carbonate and 50 mg FITC. The reaction mixture was stirred continuously for 24 hr at 37°C in a closed amber bottle. After 24 hr the reaction mixture was dialyzed in the dark (4°C) against frequent changes of 2.0 L volumes of 0.1 M potassium phosphate buffer, pH 8.0, and finally against H<sub>2</sub>O to remove salts. The dialyzed immunogen was passed over a 5.0-ml packed volume Dowex 1 × 8 column (Bio-Rad Labs, Richmond, CA) equilibrated in H<sub>2</sub>O. FITC-KLH was analyzed spectrophotometrically ( $E_M = 72,000$  M<sup>-1</sup> cm<sup>-1</sup> at 491 nm) to determine the concentration of conjugated FITC groups and by dry weight analysis for total protein concentration. Based on a molecular weight of  $1 \times 10^6$  for KLH, an average total of 207 FITC groups/KLH molecule was determined.

## 2.2. Preparative Purification of Fluorescein Ligand

Fluorescein, obtained from Molecular Probes, Inc., Eugene, OR, USA, was purified preparatively using a two-step thin-layer chromatographic system. Fluorescein dissolved in water was spotted on a silica gel 60 coated glass plate (10 × 20 cm, EM Science, Gibbstown, NJ) predried at 40°C. The first solvent system was methyl ethyl ketone (MEK) saturated with 0.01 N NaOH. Fluorescein (identified with a broad band lamp) migrated with a  $R_F$  of 0.92 in the MEK solvent. Fluorescent fluorescein was harvested from the gel and eluted in water. The harvested soluble fluorescein was spotted on a fresh silica gel plate (predried) and chromatographed in a solvent consisting of ethyl acetate (100 parts), DMF (20 parts), and 0.01 N NaOH (2 parts). Fluorescein migrated with a  $R_F$  of 0.88 in the second solvent system. Fluorescein was harvested and eluted from the silica gel with 0.1 M phosphate buffer, pH 8.0. When the eluted fluorescein was rechromatographed in either solvent system, only one fluorescent band was observed. Chromatographically purified fluorescein in pH 8.0 buffer exhibited a single exponential fluorescence lifetime of 4.02 nsec as determined by multifrequency phase and modulation fluorimetry (data not shown).

## 2.3. Immunization Protocol

Adult female albino rabbits (~4–5 kg) were immunized initially with 1.0 mg FITC-KLH emulsified in complete Freund's adjuvant. After the primary immunization all rabbits were reimmunized on days 28 and 100. Thereafter rabbits received booster immunizations every 100 days with 1.0 mg (in 200  $\mu$ l) FITC-KLH emulsified in incomplete Freund's adjuvant. The immunization regimen was continued for several months (Table I). Small bleedings were periodically obtained from the marginal ear vein during the immunization regimen to determine the persistence of the anti-fluorescein antibody response.

At designated times (Table I), relatively large bleedings were obtained from the marginal ear vein of each rabbit and processed separately (i.e., there was no pooling of individual bleedings). Antisera were immediately treated with dextran sulfate and calcium chloride to precipitate serum lipoproteins (Kranz and Voss, 1984). Lipoprotein precipitates were collected by centrifugation (10,000 rpm, 10 min at 4°C) and discarded. The soluble serum supernates were treated with 50% saturated ammonium sulfate to precipitate the gamma globulin frac-

**Table I.** Hyperimmune Rabbit Polyclonal Anti-fluorescein Fab Fragment Preparations Subfractionated by Time-dependent Dissociation Procedures

Fab Preparation	Rabbit no. <sup>a</sup>	Immune response (days) <sup>b</sup>	Age (day) <sup>c</sup>	Yield (%) <sup>d</sup>	$\lambda$ (nm) <sup>e</sup>
1.	C-8-96	880	1030	25.8	505–507
2.	C-16-97	545	695	25.8	505–507
3.	C-8-96	390	540	35.7	508–509
4.	C-1-96	910	1060	12.7	518–520
5.	C-14-98	161	311	46.4	518–520
6.	C-14-98	277	427	55.9	Both <sup>f</sup>
7.	C-14-98	378	528	84.1	505–508
8.	C-14-98	606	756	23.6	505–506
9.	C-4-97	485	635	31.5	518–520
10.	V-1	263	413	22.4	518–520
11.	C-4-97	1287	1437	18.3	Both <sup>h</sup>
12.	Control <sup>g</sup>	–	365	~0.5	–

<sup>a</sup> Adult female albino rabbits hyperimmunized with highly substituted immunogen FITC-KLH.

<sup>b</sup> Total elapsed time in days from the date of the primary immunization (see the section on Materials and Methods).

<sup>c</sup> Total age of rabbits in days at time of the bleeding.

<sup>d</sup> Percent yields of active Fab fragments based on the sum total of fragments present in each subfraction (i.e., 0.1, 1.0, 10, 100 days and the guanidine elution). The total includes the amount of protein present in all fractions and respective washes relative to the amount of Fab fragments incubated initially with the adsorbent.

<sup>e</sup> Represents the predominant absorbance peak maximum characterizing the antibody-bound fluorescein ligand in all four subfractions. As described in Table II, some minor transitions were noted as shoulders in the scans (400–600 nm) of specific subfractions. Free fluorescein in pH 8.0 buffer showed  $\lambda_{max}$  of 491 nm (see Table II).

<sup>f</sup> The 0.1- and 1.0-day elutions show an absorption maxima of 505 nm, while the 10- and 100-day elutions show a maxima of 518 nm.

<sup>g</sup> Normal (i.e., nonimmunized) adult rabbit was 1 year old at the time of the bleeding.

<sup>h</sup> The 0.1- and 1.0-day elutions show an absorption maxima of 518 nm, while the 10- and 100-day elutions show a maxima of 506 nm.

tion. After centrifugation (10,000 rpm, 10 min at 4°C) and dissolution of the precipitate in pH 8.0 buffer, the ammonium sulfate precipitation step was repeated. Final precipitates were collected by centrifugation and dissolved in 0.1 M phosphate buffer, pH 8.0. Soluble enriched gamma globulin fractions were passed over a calibrated molecular sieve column (ACA-34; 80 cm × 2 cm) equilibrated in pH 8.0 buffer to obtain purified IgG.

#### 2.4. Enzymatic Preparation of Fab Fragments

Purified IgG was dialyzed against pepsin digestion buffer (0.1 M acetate, pH 5.0). Pepsin (Sigma Chemical Co., St. Louis, MO) was added to the IgG on a 1:30 (wt/wt) basis. Proteolytic digestion proceeded for 6 hr at 37°C with constant slow rotation. The digestion mixture was immediately placed on ice and neutralized with additions of 1.0 M phosphate buffer, pH 8.0. An equal volume of saturated ammonium sulfate was added (incubated overnight at 4°C) to selectively precipitate the F(ab)<sub>2</sub> fragments while pepsin remained soluble quenching proteolysis. After centrifugation (10,000 rpm, 10 min at 4°C) the precipitate was collected and dissolved in pH 8.0 buffer. Dialyzed fractions were passed over a protein A column to selectively bind undigested IgG and residual Fc fragments or peptides. Dithiothreitol (DTT) was added to a final concentration of  $1 \times 10^{-4}$  M to the F(ab)<sub>2</sub> fragments for reduction to univalent Fab fragments. Control studies performed using SDS-PAGE showed that DTT at  $1 \times 10^{-4}$  M selectively reduced disulfide bond between the 2 H chains and not H-L disulfide bonds. Fab fragments were analyzed by nonreducing SDS-PAGE to determine purity. A single band with a molecular weight of 50 kDa was observed in all cases (data not shown). Yields of Fab fragments ranged from 40% to 61.8% of the digested IgG population. Based on a molecular weight of 150 kDa for IgG, ~67% represented the theoretical maximum yield of Fab fragments.

#### 2.5. Immunoabsorption of Purified Fab Fragments

Purified Fab fragments were incubated with FITC-Sepharose 4B adsorbent prepared as previously described (Weidner *et al.*, 1993). To determine the Fab binding capacity of the FITC-adsorbent a preparation of high-affinity anti-fluorescein Fab fragments, in which the concentration of active protein had been previously determined, were titrated against varying amounts (i.e., packed volume) of adsorbent. Upon reaching saturation it was determined that 1.0-ml packed volume of FITC-adsorbent bound 14.5 mg active Fab fragments. Based on

this value (i.e., 14.5 mg/1.0 ml) all experiments were conducted with an amount of adsorbent sufficient to bind the total concentration of Fab fragments (i.e., active + inactive fragments) being incubated with the adsorbent. Since the active anti-fluorescein antibodies represented only a percentage of the total Fab protein concentration, this formula ensured that the binding capacity of the adsorbent was in excess. A control study was conducted with Fab fragments derived from normal or nonimmune IgG to determine background or nonspecific binding.

Purified Fab fractions were incubated with washed FITC-adsorbent for 72 hr at 4°C with constant slow rotation. Upon completion of the incubation period the adsorbent was collected by centrifugation (5,000 rpm for 5 min at 4°C) and washed several times with cold pH 8.0 buffer. To the washed antibody-adsorbent complex was added 4.0 ml 0.05 M fluorescein dissolved in pH 8.0 buffer at 4°C. Fab dissociation was continued at 4°C with a constant slow rotation for the following successive time periods: 0.1 day, 1.0 day, 10 days, and 100 days. After each elution step the Fab-adsorbent complex was collected by centrifugation (5,000 rpm for 5 min at 4°C) and the Fab-ligand supernate saved. To the Fab-adsorbent complex 5.0-ml cold phosphate buffer, pH 8.0, was added as the first in a series of four successive washing steps. After the fourth washing step with buffer and centrifugation, 4.0 ml of 0.05 M fluorescein was added and the next incubation step initiated at 4°C. After the 100-day ligand elution step, 4.0 ml 6 M guanidine-HCl was added to the washed adsorbent for 72 hr at 4°C. Each 5.0-ml buffer-wash supernate was kept separate and dialyzed extensively against the pH 8.0 buffer. When no further ligand was detectable in the buffer dialysate the active Fab fractions (i.e., elution and washes) were passed over a Dowex 1-by-8 column (5.0-ml packed volume) to remove residual unbound ligand. In all cases, fluorescein ligand remained bound (R value) after Dowex chromatography. R represents the moles of ligand bound per mole of Fab fragment. The R values in all subfractions were ~1.0 after Dowex chromatography.

#### 2.6. Analyses of Affinity-purified Fab Fragments

Affinity-purified anti-fluorescein Fab fragments were analyzed spectrophotometrically for protein concentration ( $E^{1\%} = 13.0$  at 278 nm). All preparations were scanned for absorbance from 250 nm to 600 nm using a Beckman spectrophotometer. Antibody-bound fluorescein ligand displays a significant bathochromic shift (Klonis *et al.*, 1998; Voss *et al.*, 2001), but at the  $\lambda_{\max}$  the molar extinction coefficient remains the same

as free fluorescein (Voss, 1984). Thus at  $\lambda_{\max}$  the moles of ligand bound per mole of Fab fragment (i.e., R value) was determined.

### 2.7. Determination of Affinity Using a Fluorescence-based Dissociation Rate Assay

Pseudo-first order ligand dissociation rates were determined at 4°C as described by Herron (1984). Liganded affinity-purified Fab fragments of known concentration, 100  $\mu\text{l}$ , were added to quartz cuvettes (NSG Precision Cells, Farmingdale, NY) in the ISS PC-1 fluorimeter (ISS Inc., Champaign, IL). The volume was adjusted to 1.5 ml by rapid addition of a 20-fold excess (relative to the moles of active sites) of fluorescein amine (I). Fluorescein amine ligand was purified just prior to use with the two-step thin-layer chromatographic system previously described. Purified fluorescein amine showed a fluorescence lifetime of 90 to 100 psec as determined by the multifrequency phase and modulation method (data not shown). Increased fluorescence indicative of dissociated fluorescein was monitored with time using the ISS photon-counting PC-1 spectrofluorimeter with a direct data feed into a Dell® personal computer. Ligand dissociation constants were determined using the kinetics computer program and from the slopes of the plots utilizing

$$\ln (F_{U_m} - F_{U_t}) / (F_{U_m} - F_{U_0}) = -k_2 t$$

where  $F_{U_m}$  is the maximum fluorescence observed,  $F_{U_0}$  the initial fluorescence intensity observed,  $F_{U_t}$  the fluorescence observed at time  $t$ , and  $k_2$  the unimolecular dissociation rate constant.  $K_a = k_1/k_2$  when  $k_1$  is the bimolecular association rate. The  $k_1$  value of  $5 \times 10^6 \text{ M}^{-1} \text{ sec}^{-1}$  was used in all calculations (Swindlehurst and Voss, 1991).

### 2.8. Lifetime Data: Acquisition and Analysis

Fluorescence lifetime data were obtained using an ISS-K2 Multifrequency Phase and Modulation fluorimetry. The 488-nm line of a Spectro-Physics 2045 argon-ion laser was used as the excitation source. Fluorescence emission was viewed through a Schott 083 cut-on filter, that passes light  $>505 \text{ nm}$ ; fluorescein in 0.1 N NaOH was used as a reference standard with a lifetime of 4.02 nsec. Nonlinear least squares analysis using Globals™ was used to fit the lifetime data. The quality of fit was judged by the reduced chi square value using standard errors of 0.2 degrees and 0.004 for the phase and modulation, respectively (Gratton *et al.*, 1984).

## 3. RESULTS

### 3.1. Hyperimmune Rabbit Polyclonal Anti-fluorescein Antibody Populations

Anti-fluorescein IgG antibodies, as purified products of 11 individual bleedings derived from 6 different rabbits (Table I), were further processed and characterized in the subfractionation studies. All anti-fluorescein antibody preparations were obtained from hyperimmune rabbits spanning a timeframe of 161 to 1287 days post-primary immunization. Yields of active Fab fragments from the 11 IgG preparations ranged from 12.7% to 84.1% (Table I). These relatively high yields proved important, since adequate amounts of active Fab fragments were produced in each of the various subfractions for spectrofluorometric analyses.

### 3.2. Composition of Resolved Fab Subfractions

As previously described and reported (Voss *et al.*, 2001) the Fab heterogeneous populations were resolved into five subpopulations (0.1-, 1.0-, 10-, 100-day and the guanidine-HCl elution), the first four of which were studied in detail. Isoelectric focusing analyses of the Fab subpopulations indicated that all fractions were heterogeneous (i.e., contained multiple anti-fluorescein clones). However, comparative focusing results of the subfractions showed that the number of clones tended to decrease progressively from the 0.1-day to the 100-day fractions. For example, the 100-day subfraction contained only one or two major bands and a limited number of minor bands. The significance of the subfractions was their resolution on the basis of different dissociation times from the FITC-adsorbent. Differences in dissociation rates correlated with differences in affinities that correspondingly increased from the 0.1-day through the 100-day subfractions (Voss *et al.*, 2001). Guanidine-HCl elution fractions were not analyzed since the amount of protein denaturation due to the 6 M concentration represented potential analytical problems.

### 3.3. Bathochromic Shifts in the Absorption Properties of Fluorescein Ligand Bound to Subfractions of Fab Fragments

All absorption maxima of the antibody-bound fluorescein ligand listed in Table I indicated significant bathochromic shifts. Table II shows the analysis of two antibody populations (i.e., preparations #8 and #9) selected as being representative of each of the two ranges of bathochromic shifts.

**Table II.** Bathochromic Shifts in Absorption of Fluorescein Ligand Bound to Fab Fragments Derived from Various Polyclonal Anti-fluorescein IgG Antibodies Divided into Subpopulations Based on Differences in Time of Elution from a Specific Adsorbent

Free ligand	Absorption max (nm)	Emission max (nm) with excitation at:				$\Delta nm^a$
		470	480	488	490	
Fluorescein <sup>b</sup>	491	512	512	512	512	21.0 <sup>c</sup>
Fab Prep #8 <sup>d</sup>						
Bound Ligand						
0.1 day	505	519	519	519	519	14.0
1.0 day	505	522	522	522	522	17.0
10 days	507 (518 sh) <sup>e</sup>	532	533	532	532	25.5
100 days	508 (518 sh)	532	532	532	532	24.0
Fab Prep. #9 <sup>d</sup>						
Bound Ligand						
0.1 day	517	528	528	528	528	11.0
1.0 day	518	534	535	535	535	16.7
10 days	517 (507 sh)	528	529	528	529	11.5
100 days	517 (507 sh)	525	525	525	525	8.0

<sup>a</sup> Stroke's shift in nanometers as a difference between the emission maximum and absorption maximum.

<sup>b</sup> Purified by thin-layer chromatography using a two-step procedure described in the section on Materials and Methods. Spectra were taken in 0.1 M phosphate buffer, pH 8.0.

<sup>c</sup> Based on average of four emission maxima.

<sup>d</sup> Rabbit numbering based on descriptions and explanations in Table I.

<sup>e</sup> The number in parenthesis indicates that a shoulder (sh) of the wavelength maximum listed was associated with the predominant absorption peak (obtained by scanning from 250 to 600 nm).

A summary of data in Tables I and II indicated that in the hyperimmune state the individual rabbits exhibited heterogeneous IgG antibody anti-fluorescein active sites that produced spectral shifts from 491 nm to either the 505 to 507 nm and 518 to 520 nm ranges or both. The data further suggested that both spectral shift populations were present in a given rabbit (or bleeding) at a given time, although one spectral population or the other was often predominant during the late hyperimmune response (Fig. 1). Because it was previously demonstrated that the various subfractions differed significantly in affinity (progressing in affinity from the 0.1-day to the 100-day elutions) (Voss *et al.*, 2001) it was evident that there was no direct correlation between affinity and the two spectral shift antibody populations (see Tables II and IV).

#### 3.4. Correlation Between Spectral Populations and Fluorescence Emission Spectra

Results presented in Table II showed a correlation between the bathochromic shift range and the fluorescence emission maximum. Scanning data indicated that the fluorescence emission maxima were independent of the excitation wavelength (Table II). Fluorescence emission maxima of ~519 nm were characteristic for fluorescein ligand bound to antibody active sites, producing

a spectral shift in the range of 505 to 507 nm. Fluorescein ligand bound to antibody active sites, producing a spectral shift in the range of 518 to 520 nm yielded emission maxima of ~535 nm. The relatively small variability in the fluorescence maxima was attributed to (see 0.1- and 1.0-day fractions in preparation #8, Table II) the presence of both antibody subpopulations in varying amounts within the apparent predominant spectral shift antibody population. Thus, the emission maximum of 522 nm between the 1.0- and 0.1-day subfractions in preparation #8 was attributed to the 518- to 520-nm antibody populations "contaminating" the predominant 505- to 507-nm spectral shift populations. Similar but opposite trends were evident in the analyses of preparation #9 (Fig. 1). Thus, a pure antibody population of liganded fluorescein molecules displaying an absorption maximum of ~505 nm showed an emission maximum of 519 nm, while a pure antibody population containing fluorescein ligand with a bathochromic shift to ~518 nm exhibited an emission maximum of ~535 nm.

#### 3.5. Fluorescence Quenching Maxima

Studies were conducted to determine the degree of maximum fluorescence quenching ( $Q_{max}$ ) and to ascertain if a correlation existed between  $Q_{max}$  and the spectral shift antibody populations (i.e., either the 505–507

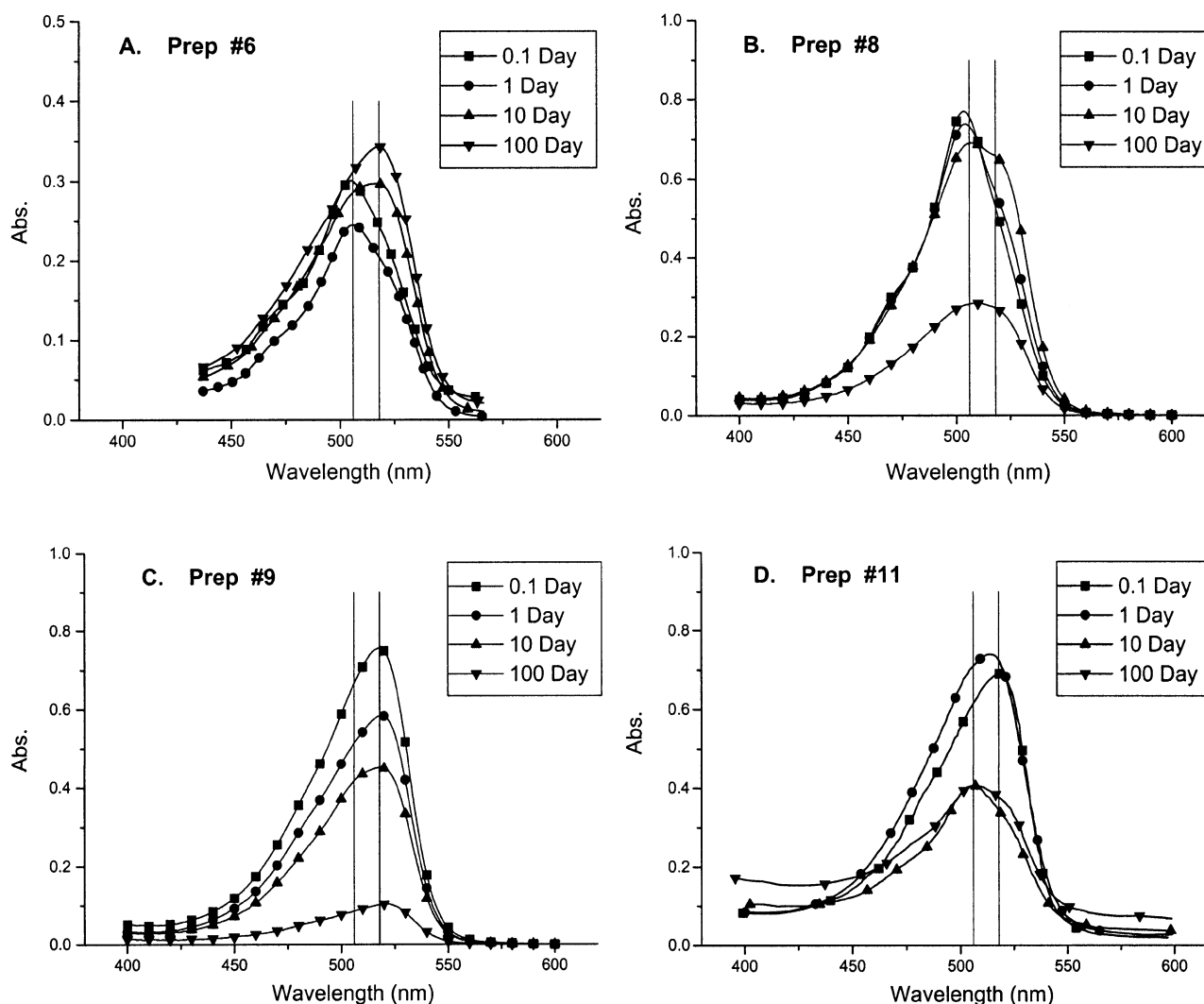


**Fig. 1.** Absorption spectra of fluorescein ligand bound to selected subpopulations of Fab fragments derived from rabbit hyperimmune anti-fluorescein IgG antibodies. Each figure contains spectra of the 0.1-day, 1.0-day, 10-day, and 100-day subfractions constituting the designated preparation. A spectrum of free fluorescein showed an absorption maximum of 491 nm. (A) Preparation #6. (B) Preparation #8. (C) Preparation #9. (D) Preparation #11. The Fab preparations are described in Table I. The vertical lines in each figure denote the 506 nm (left) and 518 nm (right) wavelengths as reference points. The spectra are not normalized for antibody or ligand concentration. Absorbance of the ligand is directly proportional to antibody protein concentration since the moles of ligand bound per mole of univalent Fab was  $\sim 1.0$  in all samples.

nm or 518–520 nm populations) or subfraction affinity (i.e., 0.1 day, 1.0 day, 10 days, or 100 days). In analyses of all 11 preparations, and their respective four subfractions listed in Table I, there were no significant trends. All antibody populations and resolved subpopulations showed similar  $Q_{\max}$  values of 95% to 97% (Table III).

### 3.6. Fluorescence Polarization

All subfractions derived from polyclonal hyperimmune anti-fluorescein antibody populations exhibited similar, if not identical, fluorescence polarization values

for the antibody-bound ligand. Polarization values ranged from 0.374 to 0.384 ( $\pm 0.002$ ) at 23°C. Free fluorescein, run as a control in all polarization studies, showed polarization values of 0.017 ( $\pm 0.002$ ) at 23°C. Thus, in all antibody populations and subfractions the fluorescein ligand was bound tightly within the antibody active site.

### 3.7. Fluorescence Lifetimes

Fab liganded subpopulations were studied by multi-frequency phase and modulation to determine the fluorescent lifetimes of the highly quenched antibody-bound

**Table III.**  $Q_{\max}$  values for Selected Fab Preparations of Polyclonal Rabbit Anti-fluorescein Antibodies

Subfraction	Fab preparation no.					
	1	2	3	5	8	9
0.1 day	95.3	96.5	96.0	95.0	96.0	97.0 <sup>a</sup>
1.0 day	95.1	96.8	96.0	95.0	96.5	97.2
10 days	95.8	97.0	96.0	94.8	96.4	97.0
100 days	96.0	97.0	96.0	95.0	96.0	97.0

<sup>a</sup> Fluorescence quenching maxima ( $Q_{\max}$ ) values determined by quantitatively comparing the fluorescence of a concentration of free fluorescein (pH 8.0) with an equivalent concentration of fluorescein ligand bound to the anti-fluorescein antibodies.

ligand. Table IV shows that the average fluorescence lifetimes of bound fluorescein ligand ranged from 0.24 to 0.30 nsec. In this study the fluorescence lifetime data obtained for the 0.1-, 1.0-, 10-, and 100-day elutions were best fit with a model having three single exponential discrete lifetime components. In this type of system, it is important to note that the fluorescence of the antibody-bound fluorescein ligand was quenched 98%, and therefore, only a small amount of free fluorescein (with a lifetime of 4.02 nsec) can make a significant fractional contribution to the fluorescence intensity relative to the quenched species. Since hapten binding to the antibody is an equilibrium process, minute levels of free fluorescein are expected; hence, the long lifetime component that appeared in the analysis was fixed to 4.02 nsec to represent this component. In addition to this component, there were two shorter lifetime components in the analysis. Both shorter components were averaged by weighting both lifetime values by their fractional contribution to the fluorescence intensity. These average lifetimes are presented in Table IV for each subfraction of preparation #9. The lifetime data showed no significant correlation with the affinities of the subfractions.

**Table IV.** Average Intrinsic Affinities and Fluorescence Lifetimes of Antibody-bound Fluorescein Ligand Associated with the Resolved Subfractions of Preparation #9

Subfraction	$K_a$ ( $M^{-1}$ ) <sup>a</sup>	Lifetime (nsec) <sup>a</sup>
0.1 day	$6.8 \times 10^9$	0.30 <sup>b</sup>
1.0 day	$2.3 \times 10^{10}$	0.24
10 days	$6.1 \times 10^{10}$	0.24
100 days	$1.3 \times 10^{11}$	0.25

<sup>a</sup> Determined at 23°C, as described in the section on Materials and Methods.

<sup>b</sup> Lifetimes measured using 488-nm excitation as described in the section on Materials and Methods. The lifetime values listed represent the average lifetimes for bound fluorescein ligand after correction for the contribution of the free ligand.

### 3.8. Subfraction Affinities

Affinities characterizing the subfractions of Fab preparation #9 are listed in Table IV. Average intrinsic affinity values ranged from  $6.8 \times 10^9 M^{-1}$  for the 0.1-day fraction to  $1.3 \times 10^{11} M^{-1}$  for the 100-day fraction. Affinity values reported in Table IV are representative of affinities for all antibody preparations analyzed. The relatively high affinities for fluorescein in all subfractions are consistent with previously cited fluorescence polarization values.

## 4. DISCUSSION

Subfractionation of polyclonal rabbit hyperimmune anti-fluorescein Fab fragments, based on differential times of dissociation from a specific adsorbent, resulted in resolution of polyclonal antibodies into affinity subgroupings (Table IV; Klonis *et al.*, 1998; Voss *et al.*, 2001). Isoelectric focusing results (not shown) indicated that the antibody subpopulations exhibited restricted heterogeneity.

In terms of the bathochromic shifts in absorption exhibited by Fab-bound fluorescein ligand, certain significant trends were evident. First, in all 11 anti-fluorescein antibody preparations studied the red shift from 491 nm (free fluorescein) corresponded to two discrete ranges, either 505 to 507 nm or 518 to 520 nm (Table I). Since the adult albino rabbits studied were not inbred and their immune responses were genetically diverse, these results indicated a basic selection phenomenon during the course of the immune response for a specific type of active site or a specific interaction within the active site. The latter is important in the context of these studies since the hyperimmune state in each rabbit was distinct, being comprised of many different anti-fluorescein antibody-producing clones or somatic mutants of parental clonal products of the time-dependent affinity maturation process (Rajewsky, 1998). The two spectral shift ranges produced by the anti-fluorescein antibody molecules were spaced by an equivalent difference in wavelengths of approximately 14 to 15 nm relative to each other and to free fluorescein (Tables II and V). Both spectral shift ranges were characteristic of the individual rabbit's immune response in general (or a given bleeding) and of the antibodies found in all four subfractions (Tables I and II). In some cases, both spectral shift antibody species were found in the same bleeding of a rabbit (Fig. 1). This finding was evidence for one spectral shift species being predominant and the other being present as an ascending or descending shoulder on the principal absorption peak (Fig. 1). In some cases the two spectral shift antibody



**Table V.** Absorption Maximum Energies and the Two Discrete Ranges of Spectral Shifts in Absorbance of Antibody-bound Fluorescein Ligand

Wavelength (nm)	Energy (kcal mol <sup>-1</sup> ) <sup>a</sup>
491	58.25
506	56.52
519	55.10
Spectra shift (nm)	Change in energy
491–506	1.73
491–51	3.15
506–519	1.42

<sup>a</sup> Energies calculated using  $E = h\nu$ , where  $\nu = c/\lambda$ ;  $c = 3 \times 10^{10}$  cm s<sup>-1</sup>;  $h$  is Planck's constant ( $1.58 \times 10^{-37}$  kcal sec/photon); Avogadro's number =  $6.03 \times 10^{23}$  photons mol<sup>-1</sup>.

species were resolved during the subfractionation process, as seen, for example, in preparation #6 where the 505 nm species was predominant in the 0.1- and 1.0-day fractions. However, while the 10-day fraction was bimodal (i.e., both spectral shift antibody species were present in nearly equal concentrations) the 100-day fraction was exclusively the 518-nm antibody species (Fig. 1). This trend of the 505-nm antibody population seemingly progressing to a 518-nm population with higher affinity was noted previously Klonis *et al.* (1998). However, in these studies the reverse transition was observed for the first time. A reverse transition was noted in preparation #11, where the 0.1- and 1.0-day subfractions were comprised of the 518-nm antibody spectral shift species while the 10- and 100-day subfractions were populated exclusively by the 506-nm antibody species (Fig. 1). Thus, the results decisively showed that the two spectral shift antibody species reflected certain common active site properties independent of affinity.

The two spectral shifts produced by the heterogeneous antibody species were independent of affinity (Tables II and IV), the degree of fluorescence quenching (i.e.,  $Q_{\max}$ ) of the bound fluorescein ligand (Table III), the fluorescence lifetimes of the antibody-bound fluorescein ligand (Table IV), and fluorescence polarization values.

One fluorescent parameter that varied directly with the spectral shift species was the fluorescence emission maximum. The 505- to 507-nm spectral shift species showed a fluorescence emission maximum of approximately 519 to 520 nm (Table II). The 518- to 520-nm species showed a fluorescence emission maximum of ~535 nm. In contrast, free fluorescein showed a fluorescence emission maximum of 512 nm. While free fluorescein showed a Stokes shift of ~21 nm, the two spectral species showed slightly smaller shifts of 15 to 17 nm

(Table II). Thus, the spectral overlap between excitation and emission was more pronounced in the liganded state.

The main question arising from these examinations of shifts in the absorption properties of antibody-bound fluorescein ligand concerns the origin, meaning, and significance of the observed discrete spectral patterns. Explanations for these observations appear to reside at the immune system and antibody active site levels based on an extensive information base regarding antibodies in general and anti-fluorescein antibodies specifically.

First, it is imperative to discuss the results of this study in the context of the hyperimmune antibody response and on the extensive antibody genetic repertoire that constitutes the mammalian immune system. The fact that only two discrete spectral shift ranges emerged from a significantly heterogeneous anti-fluorescein response alludes directly to an exquisite clonal selection process during the relatively long time period that culminated in the late hyperimmune response (Table I). One selection process that has been well documented in the rabbit anti-fluorescein response is the phenomenon of affinity maturation (Rajewsky, 1998). The latter alludes to the fact that the T-cell-dependent polyclonal immune response shows a significant increase in the average affinity with time (Steiner and Eisen, 1967). Increased affinity is attributed to preferential expansion of B-cells expressing high-affinity antibodies characterized by usage of late hyperimmune antibody variable genes. The process involves generation of somatic antibody mutants of stimulated lymphocytic clones at a high rate as a consequence of the interdependent antigenic stimulation and antigen-directed selection of high-affinity somatic mutants. Thus, with elapsed time the repertoire of germ-line encoded antibodies is changed into a repertoire of somatic mutants. Restriction in the spectral shifts observed in these studies to only two specific ranges suggested that antigen selection processes are more complex than just selection for affinity. The results indicated a preferential antigen selection process for active sites possessing specific microenvironments compatible with binding of the fluorescein ligand. Microenvironment can be defined as either a general active site property, such as hydrophobic or hydrophilic, or specific interactions (e.g., hydrogen bonds) common to all sites in the population. Based on these concepts of microenvironment the antibody active sites that produced the two spectral shift ranges possessed nearly identical microenvironments since all fluorescence parameters, except the fluorescence maxima, were identical. Distinction between the two types of antibody active sites remains unclear. It is not possible (based on the data presented) to distinguish between whether the two active sites represented two distinct

clonal lineages or that one evolved from the other during the somatic mutation process.

A second line of reasoning explaining restricted spectral shifts involves certain basic active site noncovalent bonding interactions related to anti-fluorescein specificity. This can be analyzed in part on the basis of a model murine monoclonal antibody (Mab 4-4-20) that was crystallized in the liganded state and the molecular structure determined at a resolution of less than 2.0 Å (Herron *et al.*, 1989; 1994). Mab 4-4-20 bound the dianion form of fluorescein with an affinity of  $2 \times 10^{10} \text{ M}^{-1}$ , and a  $Q_{\text{max}}$  of 96%. Fluorescein ligand bound to Mab 4-4-20 exhibited a shift in absorption to 507 nm (identical to one of the two spectral shift ranges noted in this study for the polyclonal rabbit anti-fluorescein antibodies). The emission maximum of fluorescein bound to Mab 4-4-20 was 520 nm (Klonis *et al.*, 1998), also consistent with observations characterizing the rabbit anti-fluorescein antibodies. The resolved atomic structure of Mab 4-4-20 showed that the bound fluorescein ligand resided in an aromatic "cradle" formed by tyrosines L32, H96, and H97 and tryptophans L96 and H33 deep within the active site. Since the specific aromatic residues that formed the cradle represented highly conserved intrasite residues in the primary structures of all immunoglobulins, certain cross-species corollaries were warranted. Thus, interactions similar to those in the murine site are applicable to the lapine anti-fluorescein active site. Aside from the aromatic cradle, the high affinity of  $10^{10} \text{ M}^{-1}$  was explained in part by the presence of an arginine residue at position L34. The arginine residue bonded with a negatively charged enolic group on the xanthenone aromatic ring of fluorescein. In the germ line sequence assigned to the 4-4-20 murine macromolecule, a histidine residue occupied position L34. Therefore, Mab 4-4-20 represented a somatic mutant of the germ line gene. In this analogy, the aromatic cradle appeared to provide a structural foundation for specificity and can be regarded as separate from subsequent augmented interactions that resulted from the somatic mutation process.

Either of the lines of reasoning given previously, acting dependently or independently, serves to create the microenvironment of the antibody active site. One aspect of the microenvironment that may integrate the two antigen selection processes concerns the level of hydration of the site after ligand binding, as suggested by Klonis *et al.* (1998). The microenvironment as revealed in the high-resolution crystal structure of Mab 4-4-20 in 2-methyl-2,4-pentanediol (MPD) showed that three water molecules remained in the active site after ligand binding. When 4-4-20 was crystallized in polyethylene glycol, eight water molecules occupied the site (Herron

*et al.*, 1994). Based on conclusions by Klonis *et al.* (1998) concerning the effects of solvent-water mixtures on the spectral properties of the dianion form of the fluorescein molecule, differences in the number of sequestered water molecules may have some effect in generating the two discrete bathochromic shifts observed in the rabbit anti-fluorescein system. However, no solvent water molecules in the liganded site of 4-4-20 were associated with the xanthenone portion of fluorescein. The latter is important since solvent and microenvironment effects on the carboxyl group of fluorescein do not affect the spectral properties of the molecule to any significant degree (Klonis and Sawyer, 1996). Thus, the two equally spaced discrete spectral ranges (i.e., bathochromic shifts) observed with the rabbit antibody system may reflect different degrees of hydration. Energy calculations (Table V) indicate that the differences in the various energy levels ( $\sim 1.5 \text{ kcal mol}^{-1}$ ) between the two spectral shift ranges and free fluorescein were reconcilable with various interactions or microenvironments. Differences in water content of the active site after ligand binding (i.e., a gain or loss of water molecules) may explain the two distinct ranges of shifts in the absorbance of the bound ligand. Similar energy differences have been assigned to water molecules remaining in the active site after ligand binding. Potential energies of nonbonded interactions (e.g., van der Waals contacts) involving bound fluorescein ligand and solvent fall in the range of 0.1 to 0.3  $\text{kcal mol}^{-1}$  (Herron *et al.*, 1994). Potential energies reflect the internal energy of the ligand-antibody interaction rather than free energy; however, the magnitude of the numbers are consistent with results reported in this paper. van Oss (1998) showed that the net free energy of van der Waals interactions in an antibody active site surface with an area of 3  $\text{nm}^2$  corresponded to  $-0.2$  to  $-2 \text{ kcal mol}^{-1}$ .

Solvent-water mixture studies by Klonis *et al.* (1998) also revealed that the degree of shift in the absorption of fluorescein reflected the hydrogen bonding environment (i.e., either ligand-protein or ligand-solvent). Thus, spectral shifts are an indicator of hydrogen bonding perhaps working in concert with other parameters. For example, the degree of red-shift also appeared to be attributed to a more hydrophobic antibody active site since the bathochromic shift of the fluorescein molecule bound to Mab 4-4-20 was not as large as that observed for fluorescein in anhydrous aprotic dimethyl sulfoxide (DMSO) (Klonis *et al.*, 1998). The latter suggested that hydrogen bond interactions remained in the 4-4-20 active site after ligand binding. Studies with  $\text{D}_2\text{O}$  exchange confirmed such interactions in studies with liganded Mab 4-4-20 as well as rabbit polyclonal anti-fluorescein antibodies (Kranz *et al.*, 1981). Finally, from an

energy standpoint the various values assigned to hydrogen bonds ( $1.3\text{--}3.4\text{ kcal mol}^{-1}$ ) are consistent with the  $1.5\text{ kcal mol}^{-1}$  differences in the energy values separating the two spectral shift ranges.

In summary, the observed bathochromic shifts in the absorbance of fluorescein ligand bound to specific rabbit antibodies appeared to reflect both the relative hydrophobicity of the binding sites and the presence of specific hydrogen bonds between the antibody and fluorescein ligand. Both parameters reflect the microenvironment after ligand-induced conformational changes associated with the active site (Carrero *et al.*, 1997). Thus, many anti-fluorescein clones comprising the heterogeneous rabbit antibody active site populations possess affinities that differ by several-fold but produce the same or similar bathochromic shifts in the absorption of the ligand. Active sites of those antibody molecules (or populations) that gave rise to the two discrete ranges in the shift must differ in only subtle ways. Each antibody active site can accommodate extensive intrasite amino acid changes (i.e., somatic mutations) that result in a significant enhancement in affinity but with no accompanying change in the degree of bathochromic shift associated with bound fluorescein ligand. The antibody active sites, due to differences in perhaps nonaffinity-related amino acid residues may possess slightly different levels of hydration (i.e., only one or two water molecules), hydrogen bonds, and/or subtle differences in ligand-induced conformations that may also influence hydration through differential accessibility of the aqueous environment with the bound ligand (Frauenfelder *et al.*, 1988; Carrero *et al.*, 1997). Finally, the bathochromic shift parameter is a sensitive marker for certain general requisite microenvironment features within the liganded antibody active site, together with some subtle relatively low-energy factors such as levels of hydration or hydrogen bonding interactions.

## REFERENCES

- Bailey, M. P., Hagmar, P. P., Millar, D. P., Davidson B. E., Tong, G., Haralambidis, J., and Sawyer, W. H. (1995). *Biochemistry* **34**, 15802–15812.
- Carrero, J., Mummert, M., Mallender, W. D., and Voss, E. W. Jr. (1997). *Comments Mol. Cell. Biophys.* **9**, 49–86.
- Choi, M. F. and Hawkins P. (1995). *Anal. Chim. Acta* **309**, 27–34.
- Fleming, G. R., Knight, A. W. E., Morris, J. M., Morrison, R. J. S., and G. W. Robinson, G. W. (1977). *J. Am. Chem. Soc.* **99**, 4306–4311.
- Frauenfelder, H., Parak, F., and Young, R. D. (1988). *Ann. Rev. Biophys. Chem.* **17**, 451–479.
- Gratton, E., Jameson, D. M., and Hall, R. D. (1984). *Ann. Rev. Biophys. Bioengr.* **13**, 105–124.
- Hadjianestis, J. and Nikokavouras, J. (1993). *J. Photochem. Photobiol.* **A69**, 337–343.
- Harris, D. C. and Bertolucci, M. D. (1978). *Symmetry and Spectroscopy*. Dover Publications, New York, pp. 1–4.
- Herron, J. N. (1984) In *Fluorescein Hapten: An Immunological Probe* (Voss, E. W. Jr., ed.), CRC Press, Boca Raton, FL, pp. 49–76.
- Herron, J. N., X-Min, He, Mason, M. L., Voss, E. W. Jr., and Edmundson, A. B. (1989). *Proteins* **5**, 271–280.
- Herron, J. N., Terry, A., Johnston, S., X-Min, He, Guiddat, L., Voss, E. W. Jr., and Edmundson, A. B. (1994). *Biophys. J.* **67**, 2167–2183.
- Jameson, D. M. (1984). In *Fluorescein Hapten: An Immunological Probe* (Voss, E. W. Jr., ed.), CRC Press, Boca Raton, FL, pp. 23–48.
- Kamlet, M. J. and Taft, R. W. (1976). *J. Am. Chem. Soc.* **98**, 377–383.
- Klonis, N. and Sawyer, W. H. (1996). *J. Fluoresc.* **6**, 147–157.
- Klonis, N., Clayton, A. H. A., Voss, E. W. Jr., and Sawyer, W. H. (1998). *Photochem. Photobiol.* **67**, 500–510.
- Klonis N. and Sawyer, W. H. (2000). *Photochem. Photobiol.* **72**, 179–185.
- Kranz, D. M., Herron, J. N., Giannis, D. E., and E. W. Voss Jr. (1981). *J. Biol. Chem.* **256**, 4433–4438.
- Kranz, D. M. and Voss, E. W. Jr. (1984). In *Fluorescein Hapten: An Immunological Probe* (Voss, E. W. Jr., ed.), CRC Press, Boca Raton, FL, p. 18.
- Lakowicz, J. R. (1999a). *Principles of Fluorescence Spectroscopy*, 2nd ed., Kluwer Academic, New York, Chapt.1 pp. 1–23.
- Lakowicz, J. R. (1999b). *Principles of Fluorescence Spectroscopy*, 2nd ed., Kluwer Academic, New York, Chapt. 7, pp. 211–236.
- Lindqvist, L. (1960). *Arkiv. Kem.* **16**, 79–138.
- MacGregor R. B. and Weber, G. (1981). *Ann. N.Y. Acad. Sci.* **366**, 140–150.
- Magde, D., Rojas, G. E., and Seybold, P. G. (1999). *Photochem. Photobiol.* **70**, 737–744.
- Martin, M. M. (1975). *Chem. Phys. Lett.* **35**, 105–111.
- Martin, M. and Lindqvist, L. (1975). *J. Luminesc.* **10**, 381–390.
- Mummert, M. E. and Voss, E. W. Jr. (1995). *Mol. Immunol.* **32**, 1225–1233.
- Rajewsky, K. (1998). *Encyclopedia of Immunology*, 2nd ed. (Delves, P. J. and Roitt, I. M., eds.), Academic Press, London, Vol. 1, pp. 52–54.
- Sjoback, K., Nygren, R. J., and Kubista, M. (1995). *Spectrochim. Acta A* **51**, 17–21.
- Stanton S. G., Kantor, A. B., Petrossian, A., and Owicki, J. C. (1984). *Biochim. Biophys. Acta* **776**, 228–236.
- Steiner, L. A. and Eisen, H. N. (1967). *J. Exper. Med.* **126**, 1161–1183.
- Swindlehurst, C. A. and Voss, E. W. Jr. (1991). *Biophys. J.* **59**, 619–628.
- van Oss, C. J. (1998). *Encyclopedia of Immunology*, 2nd ed. (Delves, P. J. and Roitt, I. M., eds.), Academic Press, London, Vol. 1, pp. 163–167.
- Voss, E. W. Jr. (1984). In *Fluorescein Hapten: An Immunological Probe* (Voss, E. W. Jr., ed.), CRC Press, Boca Raton, FL, pp. 3–14.
- Voss, E. W. Jr. (1990). *Comments Mol. Cell. Biophys.* **6**, 197–221.
- Voss, E. W. Jr., Croney, J. C., and Jameson, D. M. (2001). *Mol. Immunol.* **38**, 35–44.
- Watt, R. M. and Voss, E. W. Jr. (1997). *Immunochimistry* **14**, 533–541.
- Weidner, K. M., Denzin, L. K., Kim, M. L., Mallender, W. D., Miklasz, S. D., and Voss, E. W. Jr. (1993). *Mol. Immunol.* **30**, 1003–1011.
- Yguerabide, J., Talavera, E., Alvarez, J. M., and Quintero, B. (1994). *Photochem. Photobiol.* **60**, 435–441.